

Hybrid methodology for parameter algebraic identification in spatial/time domain for switched reluctance motors

Carlos Vergara-Ramírez¹, John Cortés-Romero², Horacio Coral-Enriquez³

¹Facultad de Ingeniería Mecatrónica, Escuela Tecnológica Instituto Técnico Central, Bogotá D.C., Colombia

²Departamento de Ingeniería Eléctrica y Electrónica, Facultad de Ingeniería, Universidad Nacional de Colombia, Bogotá D.C., Colombia

³Ingeniería Mecatrónica, Facultad de Ingeniería, Universidad de San Buenaventura, Bogotá D.C., Colombia

Article Info

Article history:

Received Sep 6, 2024

Revised Feb 19, 2025

Accepted Mar 11, 2025

Keywords:

Algebraic identification

Off-line estimation

On-line estimation

Parameter identification

Switched reluctance motor

ABSTRACT

The switched reluctance motor (SRM) has attracted attention in recent decades, due to its robustness, low manufacturing cost, and other performance characteristics. Thanks to the accepted and widely used mathematical model of this motor, model-based controllers, whose main foundation is the precise knowledge/identification of the motor parameters, are frequently reported in the literature and required in the industry. This article proposes a parametric identification for switching reluctance motors under an algebraic approach. The identification is based on the unsaturated model of the motor whose electrical parameters depend on the angular position. This work proposes an adaptation of the classic identification method defined in the spatial and temporal domains, due to the angular dependence on the electrical parameters and the temporal dependence on the mechanic parameters. In addition, the proposed identification strategy is simulated and experimentally validated in a DSP-based test bench. Reduced identification times, low error rates, and non-dependence of tuning parameters were obtained.

This is an open access article under the [CC BY-SA](https://creativecommons.org/licenses/by-sa/4.0/) license.



Corresponding Author:

Carlos Vergara-Ramírez

Facultad de Ingeniería Mecatrónica, Escuela Tecnológica Instituto Técnico Central

Calle. 13 No. 16-74, Bogotá D.C., Colombia

Email: cfvergarar@itc.edu.co

1. INTRODUCTION

Advancements in signal processing and control techniques have made some previously overlooked electric machines, like the switched reluctance motor (SRM), a viable option for high-performance applications. Historically, direct current (DC) motors dominated motion systems, but alternating current (AC) motors are now prevalent in robotics due to their robust structure, lower manufacturing costs, and minimal maintenance [1]. Although SRM was less favored for decades, its simple construction, efficiency, and wide speed range have reignited interest in recent years [2], [3]. In the automotive sector, SRM has become particularly attractive due to the rising cost and supply constraints of rare-earth materials essential for permanent magnet motors. This challenge makes SRM a competitive alternative for electric vehicle production [4], [5].

Numerous motor identification strategies have been proposed, aiding in model-based controller design and motor development [6], [7]. Both heuristic and deterministic methods allow parameter estimation, either offline or online [8], [9]. Notably, SRM parametric identification has been reported with various techniques, including neural networks and fuzzy logic, many of which rely on heuristic tuning [10], [11]. A significant number of approaches focus on current versus flux or angle versus inductance estimations,

overlooking other important parameters like resistance, friction, and inertia [12]. These strategies often require large data tables, increasing memory demands in embedded systems.

Recent studies propose online identification methods embedded in the control loop to estimate SRM parameters [13], although their convergence is often dependent on process dynamics. There is thus a need for identification strategies that can operate both in open and closed-loop configurations, with improvements in convergence and error reduction [14], [15]. The algebraic identification method proposed in this work builds on the approach detailed in [16], offering precision and fast convergence for linear and nonlinear systems, and successfully implemented in various control loops [17], [18].

In the context of SRM, electrical parameter identification poses a unique challenge due to the complex inductance matrix. This is particularly true for motors with fewer poles, where inductance depends strongly on angular displacement and exhibits periodicity [19]. The proposed methodology addresses this by combining spatial and temporal domain strategies to enhance the accuracy and speed of the identification process. The spatial domain approach has shown success in systems where electrical or mechanical dynamics are spatially dependent [20], offering new possibilities for better identification and control in various fields. The contributions of this paper include:

- Full identification of SRM parameters, including both mechanical and electrical components.
- A hybrid algebraic method using spatial and temporal domains for improved accuracy and speed.
- Experimental and simulation results demonstrating reduced convergence time and low parametric error.
- A parameter-free tuning strategy that simplifies implementation.
- Compatibility for both online and offline use.

This paper is organized as follows. Section 2, method presents the identification strategy, the SRM model, and practical implementation details. Section 3, results and discussion, analyzes the outcomes of simulations and experimental tests. Finally, section 4, conclusion, provides the concluding remarks and highlights the key findings.

2. METHOD

This section presents the strategy for estimating electrical and mechanical parameters in a SRM using an algebraic approach and some practical aspects to evaluate the proposal.

2.1. Identification strategy

Figure 1 represents the proposed identification strategy, which is divided into two phases. The first phase involves identifying the electrical parameters, which is carried out in the spatial domain. Once the inductance function is identified, the induced torque can be estimated, enabling the second phase, which corresponds to estimating mechanical parameters in the temporal domain. This domain change requires sampling the variables in each domain experimentally. Specifically, for the spatial domain, the encoder provides the sampling clock signal. The open-loop control applies a fixed voltage to the corresponding phase, ensuring continuous angular displacement, making position measurement essential. To detail the proposed strategy, the SRM model is briefly presented:

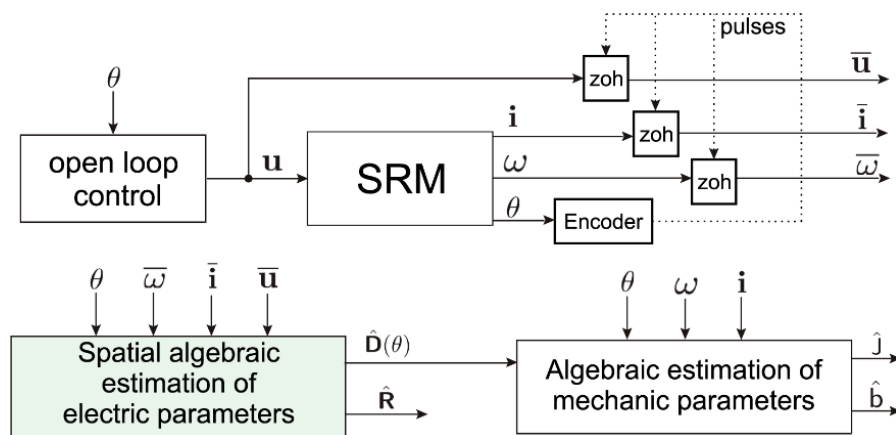


Figure 1. Strategy proposed for SRM identification

2.1.1. Dynamic model of the switched reluctance motor

The structure of a SRM, shown in Figure 2, consists of salient poles on both the stator and rotor. Opposing stator poles share a winding of the same phase, and rotor movement occurs when winding excitation causes the poles to align, maximizing magnetic flux. The motor depicted is a 4/2 SRM configuration, with four stator poles and two rotor poles, corresponding to two phases.

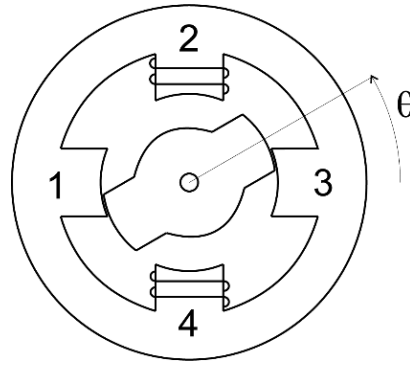


Figure 2. SRM 4/2

This SRM model is widely accepted and experimentally validated. It assumes that the stator phases are magnetically uncoupled, with negligible mutual inductance [21]. Omitting saturation and friction, the SRM dynamics are governed by the following (1) to (3) [22]:

$$\dot{\theta}(t) = \omega(t) \quad (1)$$

$$J\dot{\omega}(t) = \frac{1}{2}i^T(t)C(\theta)i(t) - b\omega(t) - \tau_L(t) \quad (2)$$

$$D(\theta)\frac{di(t)}{dt} = u(t) - \omega(t)C(\theta)i(t) - Ri(t) \quad (3)$$

For an N-phases motor, $u = [u_1, u_2, \dots, u_N]^T$ and $i = [i_1, i_2, \dots, i_N]^T$ are the phase voltage and current vectors, θ is the rotor's angular position, τ_L is the load torque, J is total inertia (rotor and load), b is the viscous friction coefficient, while $D(\theta)$ and R represent the inductance and resistance matrices:

$$D(\theta) = \text{diag} [f_1(\theta), f_2(\theta), \dots, f_N(\theta)] \quad (4)$$

$$R = \text{diag} [r_1, r_2, \dots, r_N] \quad (5)$$

with $C(\theta) = \frac{dD(\theta)}{d\theta}$. The variable $f_j(\theta)$ is the inductance of phase j ($j = 1, \dots, N$), periodic with a period $2\pi/N_r$, where N_r is the rotor pole count. Using a Fourier series approximation:

$$f_j(\theta) = l_{j0} - \sum_{p=1}^{\infty} \left\{ l_{jp}^s \sin \left[pN_r\theta - (j-1)\frac{2\pi}{N} \right] + l_{jp}^c \cos \left[pN_r\theta - (j-1)\frac{2\pi}{N} \right] \right\} \quad (6)$$

where l_{jp}^s to l_{jp}^c are inductance coefficients.

Lastly, the torque generated by the SRM τ exhibits semi-periodicity, depending on rotor pole count and phase currents, following (7):

$$\tau = \frac{1}{2}i^T(t)C(\theta)i(t) \quad (7)$$

2.1.2. Electrical parameters identification

Given the structure of the inductance matrices (C and D), the dependence on angular displacement is evident in the mathematical model described. Regardless of the asymmetries in the SRM's construction, the behavior of the associated magnetic reluctance is repeated in each rotation.

An angular domain representation of the electric and magnetic dynamics makes the terms periodic over a defined angular period. Therefore, its representation in the time domain is affected by both position and speed. This angular dependence motivates a spatial domain approach to algebraic identification. In (3), which represents current dynamics in the temporal domain, can be transformed into the spatial domain using the following definition [20]:

$$\frac{df(t)}{dt} = \frac{d\theta}{dt} \frac{df(\theta)}{d\theta} = \bar{\omega} \frac{df(\theta)}{d\theta} \quad (8)$$

Applying this transformation to (3), we obtain:

$$D(\theta) \frac{d\bar{i}}{d\theta} + C(\theta)\bar{i} + R\vartheta_1(\theta) = \vartheta_2(\theta) \quad (9)$$

where,

$$\vartheta_1(\theta) = \frac{1}{\bar{\omega}} \bar{i}, \quad \vartheta_2(\theta) = \frac{1}{\bar{\omega}} \bar{u} \quad (10)$$

Using the chain rule and reorganizing terms, this becomes:

$$\frac{d}{d\theta} \beta(\theta) + R\vartheta_1(\theta) = \vartheta_2(\theta) \quad (11)$$

with

$$\beta(\theta) = D(\theta)\bar{i} \quad (12)$$

Applying the Laplace transform to this equation for algebraic treatment gives:

$$\bar{s}B(\bar{s}) - \beta(0) + RV_1(\bar{s}) = V_2(\bar{s}) \quad (13)$$

Differentiating with respect to the Laplace variable \bar{s} to eliminate initial conditions:

$$B(\bar{s}) + \bar{s} \frac{d}{d\bar{s}} B(\bar{s}) + R \frac{d}{d\bar{s}} V_1(\bar{s}) = \frac{d}{d\bar{s}} V_2(\bar{s}) \quad (14)$$

Multiplying by \bar{s}^{-1} and returning to the spatial domain results in an integral relationship:

$$\int_0^\theta \beta(\lambda) d\lambda - \theta\beta - R \int_0^\theta \lambda\vartheta_1(\lambda) d\lambda = - \int_0^\theta \lambda\vartheta_2(\lambda) d\lambda \quad (15)$$

According to Loría *et al.* [23], it is feasible to approximate (6) using a single harmonic for motors with more than two phases. However, the 4/2 motor used in this validation achieves an accurate approximation using the following inductance function:

$$f_j = l_{j0} - l_{j1}^s \sin(2\theta) - l_{j1}^c \cos(2\theta) - l_{j2}^s \sin(4\theta) - l_{j2}^c \cos(4\theta) \quad (16)$$

Thus, (15) for phase j becomes:

$$l_{j0}p_{j1} + l_{j1}^s p_{j2} + l_{j1}^c p_{j3} + l_{j2}^s p_{j4} + l_{j2}^c p_{j5} + r_j p_{j6} = q_j \quad (17)$$

where,

$$p_{j1}(\theta) = \int_0^\theta i_j(\lambda) d\lambda - \theta i_j \quad (18)$$

$$p_{j2}(\theta) = - \int_0^\theta i_j(\lambda) \sin(2\lambda) d\lambda + \theta i_j \sin(2\theta) \quad (19)$$

$$p_{j3}(\theta) = - \int_0^\theta i_j(\lambda) \cos(2\lambda) d\lambda + \theta i_j \cos(2\theta) \quad (20)$$

$$p_{j4}(\theta) = - \int_0^\theta i_j(\lambda) \sin(4\lambda) d\lambda + \theta i_j \sin(4\theta) \quad (21)$$

$$p_{j5}(\theta) = - \int_0^\theta i_j(\lambda) \cos(4\lambda) d\lambda + \theta i_j \cos(4\theta) \quad (22)$$

$$p_{j6}(\theta) = - \int_0^\theta \lambda \vartheta_{j1}(\lambda) d\lambda, \quad q_j(\theta) = - \int_0^\theta \lambda \vartheta_{j2}(\lambda) d\lambda \quad (23)$$

This can be represented as a linear system:

$$P_j \Theta_j = q_j, \quad (24)$$

where,

$$P_j = [p_{j1} \quad p_{j2} \quad p_{j3} \quad p_{j4} \quad p_{j5} \quad p_{j6}] \quad (25)$$

$$\Theta_j = [l_{j0} \quad l_{j1}^s \quad l_{j1}^c \quad l_{j2}^s \quad l_{j2}^c \quad r_j]^T \quad (26)$$

The electrical parameters of each phase, including resistance and inductance function coefficients Θ_j , are determined by solving the linear system in (24). The required variables include current, voltage, speed, and position. Next, we present the strategy for identifying mechanical parameters under the same algebraic approach.

2.1.3. Mechanical parameters identification

Based on the mechanical model of the SRM given in (1) and (2), without considering the load torque and deriving once with respect to time to eliminate constant uncertainties, we obtain:

$$J \ddot{\omega} = \dot{u}_\tau - b \dot{\omega} \quad (27)$$

Applying the algebraic procedure in the frequency domain, the Laplace transform results in:

$$J[s^2 W(s) - s\omega(0) - \dot{\omega}(0)] = sU_\tau(s) - u_\tau(0) - b[sW(s) - \omega(0)] \quad (28)$$

Differentiating twice with respect to s , to eliminate initial conditions for speed, acceleration, and torque, leads to:

$$J \left[2W(s) + 4s \frac{dW(s)}{ds} + s^2 \frac{d^2 W(s)}{ds^2} \right] + b \left[2 \frac{dW(s)}{ds} + s \frac{d^2 W(s)}{ds^2} \right] = 2 \frac{dU_\tau(s)}{ds} + s \frac{d^2 U_\tau(s)}{ds^2}. \quad (29)$$

Multiplying both sides by s^2 and applying the inverse Laplace transform results in the following integral relation:

$$J p_1(t) + b p_2(t) = q_m(t) \quad (30)$$

This can be written as a linear combination:

$$P_m \Theta_m = q_m \quad (31)$$

where,

$$P_m = [p_1 \quad p_2], \quad \Theta_m = [J \quad b]^T \quad (32)$$

with:

$$p_1(t) = 2 \int_0^t \int_0^\lambda w(\lambda_1) d\lambda_1 d\lambda - 4 \int_0^t \lambda w(\lambda) d\lambda + t^2 w \quad (33)$$

$$p_2(t) = -2 \int_0^t \int_0^\lambda \lambda_1 w(\lambda_1) d\lambda_1 d\lambda + \int_0^t \lambda^2 w(\lambda) d\lambda \quad (34)$$

$$q_m(t) = -2 \int_0^t \int_0^\lambda \lambda_1 u_\tau(\lambda_1) d\lambda_1 d\lambda + \int_0^t \lambda^2 u_\tau(\lambda) d\lambda \quad (35)$$

The parameters J and b are obtained by solving (31). For this process, it is necessary to acquire the phase currents, position, and speed, in addition to estimating the torque generated by the motor using the identified inductance matrix $D(\theta)$ and (7).

2.2. Practical aspects for algebraic identification

To solve numerically (24) and (31), we can estimate the parameters vector $\hat{\theta}$ using the least squares method, which minimizes the integral of the quadratic error:

$$J(\theta, x) = \frac{1}{2} \int_0^x \varepsilon^2(\theta, \lambda) d\lambda \quad (36)$$

where the residual error is defined as (37):

$$\varepsilon(\theta, x) = P(x)\theta - q(x) \quad (37)$$

and the estimate is:

$$\hat{\theta} = \arg\{\min_{\theta} J(\theta, x)\} \quad (38)$$

with x being θ for electrical parameters and t for mechanical ones. The analytical solution is given by (39):

$$\hat{\theta} = \left[\int_0^x P^T(\lambda)P(\lambda)d\lambda \right]^{-1} \int_0^x P^T(\lambda)q(\lambda)d\lambda \quad (39)$$

2.2.1. Parametric error index

The sensitivity index measures how the residual error changes when a specific parameter varies:

$$\Delta\hat{\theta} = \sqrt{J(\hat{\theta}, t)(M_{pp(i,i)}^{-1})} \quad (40)$$

indicating the maximum parameter variation without doubling the error. A smaller index implies better estimation quality. Where $M_{pp} = \int_0^x P^T(\lambda)P(\lambda)d\lambda$ and $M_{pp(i,i)}^{-1}$ is the corresponding value to the component of position (i, i) from M_{pp}^{-1} .

2.2.2. Numerical solution

Following [24], QR factorization is employed for solving (39), providing computational efficiency for real-time applications.

– Numerical integration

The integral of $f(x)$:

$$I(x) = \int_0^x f(\lambda)d\lambda \quad (41)$$

was computed via Euler's method:

$$I(k\Delta_x + \Delta_x) = I(k\Delta_x) + \Delta_x f(k\Delta_x), \quad (42)$$

with $\Delta_\theta = \pi/500$ for the spatial domain and $\Delta_t = 100\mu s$ for the temporal domain. The next section presents both simulation and experimental results using the proposed strategy, Figure 1.

3. RESULTS AND DISCUSSION

The mechanical and electrical parameter identification strategies were validated through both simulation and experimental processes, using open-loop control for the SRM. Current, voltage, position, and speed signals were acquired, and (24), (31), and (39) were applied to calculate the parameters.

3.1. Practical aspects for algebraic identification

Reference values for the inductance matrix $D(\theta)$ and resistance matrix R were measured using an RLC instrument (*PM6306*, FLUKE), varying the rotor's angular position. The results of these direct measurements are listed in the second column of Table 1.

Using Simulink® and MATLAB®, the parametric identification process was simulated for ten inductance function coefficients, two-phase resistances, inertia, and viscous friction coefficient. Figure 3 and Table 1 shows the simulated results, mechanical parameter estimation began 0.2 s later, as it depends on the inductance matrix.

Table 1. Simulation results of the proposed strategy

SRM parameter	Assigned value, θ	Estimated value, $\hat{\theta}$	Parametric error, $\Delta\hat{\theta}$
l_{10}	8.07×10^{-3}	8.15×10^{-3}	1.61×10^{-5}
l_{20}	8.09×10^{-3}	8.25×10^{-3}	1.72×10^{-5}
l_{11}^s	7.22×10^{-3}	7.22×10^{-3}	1.32×10^{-5}
l_{21}^s	-7.30×10^{-3}	-7.39×10^{-3}	1.49×10^{-5}
l_{11}^c	-3.79×10^{-3}	-3.73×10^{-3}	1.60×10^{-5}
l_{21}^c	3.82×10^{-3}	3.87×10^{-3}	1.54×10^{-5}
l_{12}^s	1.54×10^{-3}	1.53×10^{-3}	8.42×10^{-6}
l_{22}^s	1.58×10^{-3}	1.59×10^{-3}	6.85×10^{-6}
l_{12}^c	1.69×10^{-3}	1.65×10^{-3}	1.05×10^{-5}
l_{22}^c	1.84×10^{-3}	1.82×10^{-3}	8.78×10^{-6}
r_1	2.56	2.56	1.85×10^{-5}
r_2	2.56	2.55	1.305×10^{-5}
J	4.21×10^{-5}	4.24×10^{-5}	1.41×10^{-6}
b	2.24×10^{-4}	2.26×10^{-4}	1.34×10^{-5}

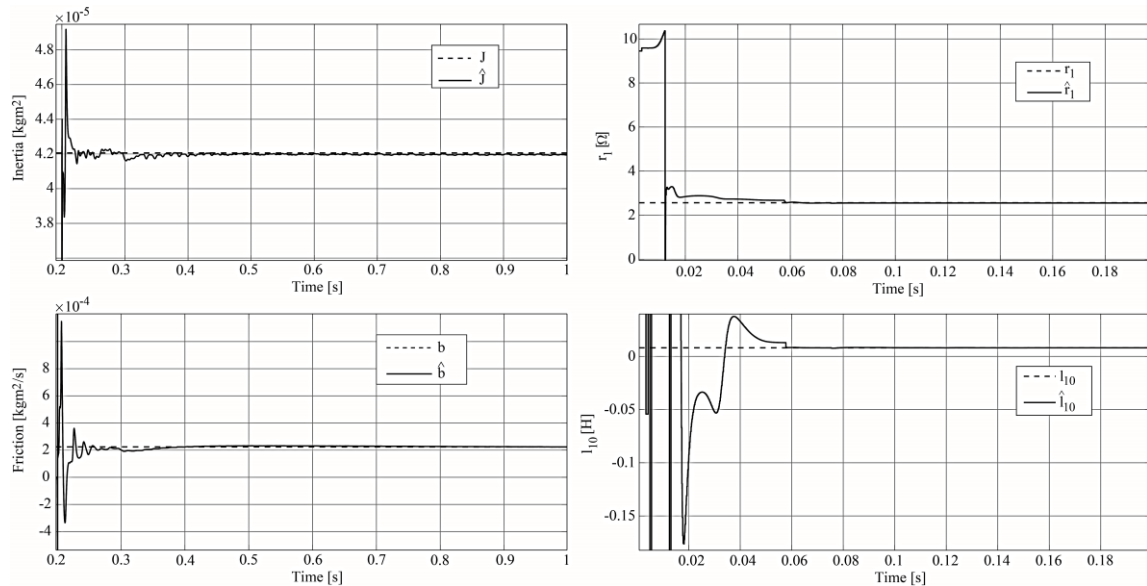


Figure 3. Results of simulation for inertia, friction, r_1 , and l_{10} parameter identification

3.2. Experimental results

A low-cost test bench was designed for signal processing, acquisition, and generation, as shown in Figure 4. The SRM was controlled via an asymmetric half-bridge power converter [25] operating at 12.5 kHz and modulating a DC source of up to 30 VDC. The acquisition circuit for current and voltage used the integrated *AMC1100* at a sampling rate of 10 kHz. The SRM used is a 4/2, 500 W motor *HSSRM-52F-50310*, coupled to a permanent magnet synchronous motor (PMSM) *AKM22E*. The real-time signal processing was handled by a *Delfino TMS320F28377S* microcontroller. The encoder resolution was set to 1000 pulses per revolution, and data were recorded on a host computer.

Data were acquired similarly to the simulation process, exciting the SRM in open loop as per Figure 1. The results were compared with the strategy in [14], which used parameters $\lambda = 50$, $\beta = 0.6$, and $P_0 = 0.6I$. In Figure 5, the inertia and friction parameter identification results are shown. Table 2 presents the results, along with their error indices, comparing them with [14].

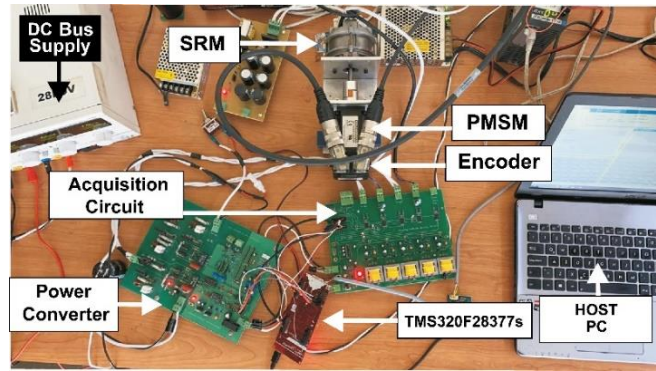


Figure 4. Test-bed used to validate the proposed strategy

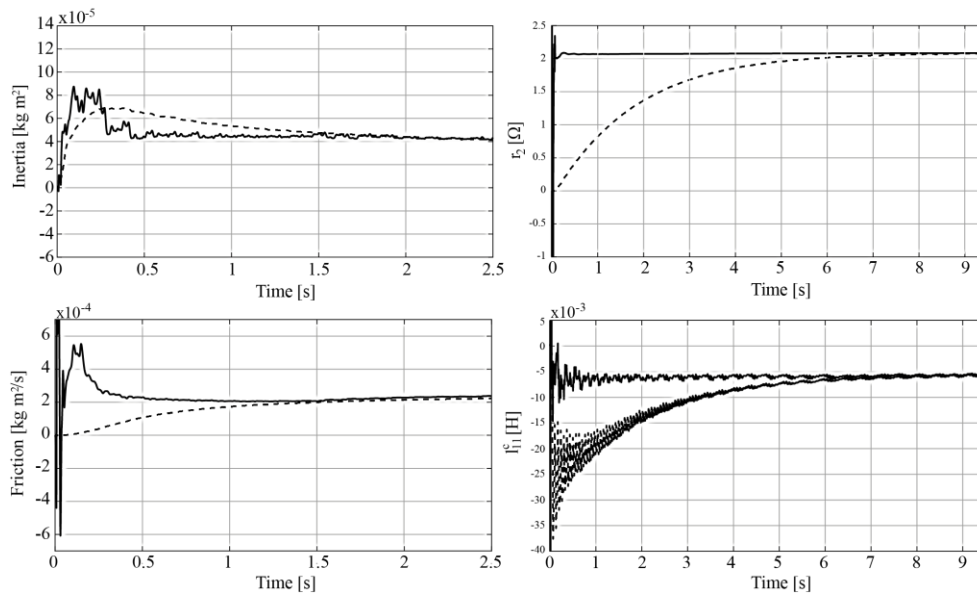
Figure 5. Experimental estimation of inertia, friction, r_1 and l_{11}^c : solid line signal from the proposed strategy, dashed line signal from [14]

Table 2. Experimental results of the proposed strategy and [14]

SRM parameter	Estimated value, $\hat{\theta}$	Parametric error, $\Delta\hat{\theta}$	Estimated value with [14] $\hat{\theta}_A$	Parametric error with [14] $\Delta\hat{\theta}_A$
l_{10}	10.2×10^{-3}	5.16×10^{-2}	9.93×10^{-3}	1.23×10^{-1}
l_{20}	9.99×10^{-3}	4.71×10^{-2}	9.57×10^{-3}	1.39×10^{-1}
l_{11}^s	9.14×10^{-3}	5.35×10^{-2}	8.82×10^{-3}	1.31×10^{-1}
l_{21}^s	-9.28×10^{-3}	4.85×10^{-2}	-8.84×10^{-3}	1.47×10^{-1}
l_{11}^c	-5.36×10^{-3}	5.81×10^{-2}	-5.50×10^{-3}	1.37×10^{-1}
l_{21}^c	5.92×10^{-3}	5.28×10^{-2}	6.03×10^{-3}	1.53×10^{-1}
l_{12}^s	2.14×10^{-3}	3.39×10^{-2}	2.29×10^{-3}	8.24×10^{-2}
l_{22}^s	2.33×10^{-3}	3.06×10^{-2}	2.53×10^{-3}	9.17×10^{-2}
l_{12}^c	1.59×10^{-3}	1.41×10^{-2}	1.56×10^{-3}	4.14×10^{-2}
l_{22}^c	1.93×10^{-3}	1.36×10^{-2}	1.82×10^{-3}	4.57×10^{-2}
r_1	2.08	1.46×10^{-3}	2.08	4.23×10^{-1}
r_2	2.20	1.62×10^{-3}	2.20	4.75×10^{-1}
J	4.34×10^{-5}	2.54×10^{-6}	4.13×10^{-5}	6.98×10^{-5}
b	2.22×10^{-4}	1.81×10^{-5}	2.23×10^{-4}	1.01×10^{-4}

Based on the simulation results (Table 1 and Figure 3) and experimental results (Table 2 and Figure 5), it is evident that the proposed spatial/time domain methodology effectively estimates the electrical and mechanical parameters of the SRM. In the simulation results, a rapid convergence of the estimated parameters to the assigned values is observed in less than 0.3 seconds. Similarly, the experimental results

demonstrate a fast response, with minimal variation after 1 seconds, being nearly five times faster than that reported in [14].

Regarding the parametric error indices, the simulation results show values very close to zero, with the highest index being 1.85×10^{-5} . However, in the experimental results, a considerable increase in these indices is observed, where the maximum value obtained by the proposed method is 5.81×10^{-2} . This increase could be attributed to signal noise, mechanical and electrical defects in the test-bed, discretization of temporal and spatial domains, as well as other practical phenomena that introduce uncertainty in the estimation. Nonetheless, even in terms of error indices, the proposed method proves superior, as these values are at least twice as low for any parameter compared to those obtained with [14].

The obtained simulation and experimental results confirm that the strategy can be implemented in both on-line and off-line applications, achieving fast estimations with low parametric error and no need for tuning, in comparison to other strategies like [14]. A key challenge for future work is to reduce the parametric error indices in experimental applications and to implement the strategy within an adaptive control scheme that requires online parameter estimation.

4. CONCLUSION

This study introduces a comprehensive identification methodology SRM parameters, encompassing both mechanical and electrical components. By employing a hybrid algebraic approach that combines spatial and temporal domains, the proposed method enhances identification accuracy and convergence speed, addressing key challenges in parameter estimation. Experimental and simulation results validate this methodology, demonstrating significant improvements in convergence time and minimizing parametric error compared to conventional approaches. One of the notable strengths of this method is its parameter-free tuning strategy, which simplifies implementation and reduces the need for extensive adjustments, making it practical and efficient for real-world applications. Additionally, its compatibility for both online and offline use broadens its applicability, enabling seamless integration into control loops for high-performance systems. These features collectively make this approach a valuable tool for engineers and researchers working in identification and control systems, as it meets the rigorous demands of modern applications in precision and responsiveness.

As a direction for future research, this methodology could be applied to online operations, such as adaptive control strategies, to further explore its potential in dynamic and continuously changing environments. Such applications would not only validate its robustness but also expand its utility in real-time scenarios where precision and adaptability are critical.

FUNDING INFORMATION

Authors state no funding involved.

AUTHOR CONTRIBUTIONS STATEMENT

This journal uses the Contributor Roles Taxonomy (CRediT) to recognize individual author contributions, reduce authorship disputes, and facilitate collaboration.

Name of Author	C	M	So	Va	Fo	I	R	D	O	E	Vi	Su	P	Fu
Carlos Vergara-Ramírez	✓	✓	✓	✓		✓	✓	✓	✓	✓	✓			✓
John Cortés-Romero	✓	✓			✓	✓	✓		✓	✓		✓	✓	✓
Horacio Coral-Enriquez	✓	✓	✓	✓	✓	✓	✓	✓		✓	✓		✓	✓

C : **C**onceptualization

M : **M**ethodology

So : **S**oftware

Va : **V**alidation

Fo : **F**ormal analysis

I : **I**nvestigation

R : **R**esources

D : **D**ata Curation

O : Writing - **O**riginal Draft

E : Writing - Review & **E**ditting

Vi : **V**isualization

Su : **S**upervision

P : **P**roject administration

Fu : **F**unding acquisition

CONFLICT OF INTEREST STATEMENT

Authors state no conflict of interest.

DATA AVAILABILITY

The data that support the findings of this study are available from the corresponding author, Carlos Vergara-Ramírez, upon reasonable request.

REFERENCES

- [1] S. Singh, S. N. Singh, and A. N. Tiwari, "PMSM Drives and its Application: An Overview," *Recent Advances in Electrical & Electronic Engineering (Formerly Recent Patents on Electrical & Electronic Engineering)*, vol. 16, no. 1, pp. 4–16, Feb. 2022, doi: 10.2174/2352096515666220812091445.
- [2] X. Sun, K. Diao, G. Lei, and J. Zhu, *Multi-objective Design Optimization of Switched Reluctance Motor Drive Systems*. Singapore: Springer Nature Singapore, 2024, doi: 10.1007/978-981-96-0672-6.
- [3] S. Mafrici, V. Madonna, C. M. Meano, K. F. Hansen, and A. Tenconi, "Switched Reluctance Machine for Transportation and Eco-Design: A Life Cycle Assessment," *IEEE Access*, vol. 12, pp. 68334–68344, 2024, doi: 10.1109/ACCESS.2024.3400324.
- [4] R. S. and J. R., "Review on electric mobility: Trends, challenges and opportunities," *Results in Engineering*, vol. 23, pp. 1–13, Sep. 2024, doi: 10.1016/j.rineng.2024.102631.
- [5] Y. Lan *et al.*, "Switched reluctance motors and drive systems for electric vehicle powertrains: State of the art analysis and future trends," *Energies*, vol. 14, no. 8, pp. 1–29, Apr. 2021, doi: 10.3390/en14082079.
- [6] J. Kasac, D. Kotarski, and P. Piljek, "Frequency-shifting-based algebraic approach to stable on-line parameter identification and state estimation of multirotor UAV," *Asian Journal of Control*, vol. 21, no. 4, pp. 1619–1629, Jul. 2019, doi: 10.1002/asjc.2042.
- [7] Y. A. Khan and V. Verma, "Stator resistance estimation for MRAS-based speed sensorless vector-controlled switched reluctance motor drive," *Electrical Engineering*, vol. 103, no. 4, pp. 1949–1963, 2021, doi: 10.1007/s00202-020-01203-3.
- [8] B. Jing, X. Dang, Z. Liu, J. Wang, and Y. Jiang, "Torque Ripple Reduction Of Switched Reluctance Motor Based On Neural Network Sliding Mode Parameter Online Learning," *Journal of Applied Science and Engineering*, vol. 27, no. 6, pp. 2667–2673, 2024, doi: 10.6180/jase.202406_27(6).0013.
- [9] A. Kumar and B. Singh, "Magnetic Characteristics-less Position Sensorless Control of SRM drive for a Wide Speed Range for Light Electric Vehicle," in *2023 IEEE IAS Global Conference on Renewable Energy and Hydrogen Technologies (GlobConHT)*, IEEE, Mar. 2023, pp. 1–6, doi: 10.1109/GlobConHT56829.2023.10087810.
- [10] A. Ouannou, A. Brouri, L. Kadi, and H. Oubouaddi, "Identification of switched reluctance machine using fuzzy model," *International Journal of System Assurance Engineering and Management*, vol. 13, no. 6, pp. 2833–2846, 2022, doi: 10.1007/s13198-022-01749-4.
- [11] H. Oubouaddi, A. Ouannou, L. Kadi, and A. Brouri, "Identification of switched reluctance machine inductance using artificial neural network," in *2022 2nd International Conference on Innovative Research in Applied Science, Engineering and Technology, IRASET 2022*, IEEE, Mar. 2022, pp. 1–6, doi: 10.1109/IRASET52964.2022.9737988.
- [12] A. Ouannou *et al.*, "Parameter Identification of Switched Reluctance Motor SRM Using Exponential Swept-Sine Signal," *Machines*, vol. 11, no. 6, p. 625, Jun. 2023, doi: 10.3390/machines11060625.
- [13] Y. Long and J. Du, "Adaptive Position Control Strategy of SRM-Based EMA System for Precision Position Tracking," *IEEE Transactions on Transportation Electrification*, vol. 9, no. 3, pp. 4680–4691, Sep. 2023, doi: 10.1109/TTE.2023.3243107.
- [14] M. Aguado-Rojas, P. Maya-Ortiz, and G. Espinosa-Pérez, "On-line estimation of switched reluctance motor parameters," *International Journal of Adaptive Control and Signal Processing*, vol. 32, no. 6, pp. 950–966, Jun. 2018, doi: 10.1002/acs.2877.
- [15] A. M. A. Oteafy, "Fast and Comprehensive Online Parameter Identification of Switched Reluctance Machines," *IEEE Access*, vol. 9, pp. 46985–46996, 2021, doi: 10.1109/ACCESS.2021.3068245.
- [16] J. Cortés-Romero, A. Jimenez-Triana, H. Coral-Enriquez, and H. Sira-Ramírez, "Algebraic estimation and active disturbance rejection in the control of flat systems," *Control Engineering Practice*, vol. 61, pp. 173–182, Apr. 2017, doi: 10.1016/j.conengprac.2017.02.009.
- [17] S. J. Landa-Damas *et al.*, "A Simplified Model for the On-Line Identification of Bearing Direct-Dynamic Parameters Based on Algebraic Identification (AI)," *Mathematics*, vol. 11, no. 14, p. 3131, Jul. 2023, doi: 10.3390/math11143131.
- [18] Y. Briceno-Isquierdo, L. Campos-Quesada, J. Alarcon-Jaramillo, and H. Coral-Enriquez, "Algebraic Identification Approach for Parameter Estimation in Surface-Mounted Permanent Magnet Synchronous Motors," in *Proceedings of the 2021 IEEE 5th Colombian Conference on Automatic Control, CCAC 2021*, IEEE, Oct. 2021, pp. 204–209, doi: 10.1109/CCAC51819.2021.9633290.
- [19] Z. Rayeen, A. Azeem, A. Iqbal, and S. Payami, "An Improved AC Supply based Method for Measuring the Inductance Profile of SRM Using SOGI," *IEEE Transactions on Instrumentation and Measurement*, vol. 74, pp. 1–11, 2024, doi: 10.1109/TIM.2024.3502778.
- [20] H. Coral-Enriquez and J. Cortés-Romero, "Spatial-domain active disturbance rejection control for load mitigation in horizontal-axis wind turbines," in *2016 IEEE Conference on Control Applications, CCA 2016*, IEEE, Sep. 2016, pp. 575–580, doi: 10.1109/CCA.2016.7587891.
- [21] A. De La Guerra, M. A. Arteaga-Pérez, A. Gutiérrez-Giles, and P. Maya-Ortiz, "Speed-sensorless control of SR motors based on GPI observers," *Control Engineering Practice*, vol. 46, pp. 115–128, Jan. 2016, doi: 10.1016/j.conengprac.2015.10.010.
- [22] A. Brouri, L. Kadi, A. Tounzi, A. Ouannou, and J. Bouchnaif, "Modelling and identification of switched reluctance machine inductance," *Australian Journal of Electrical and Electronics Engineering*, vol. 18, no. 1, pp. 8–20, Jan. 2021, doi: 10.1080/1448837X.2020.1866269.
- [23] A. Loria, G. Espinosa-Pérez, and E. Chumacero, "Robust passivity-based control of switched-reluctance motors," *International Journal of Robust and Nonlinear Control*, vol. 25, no. 17, pp. 3384–3403, Nov. 2015, doi: 10.1002/rnc.3270.
- [24] L. N. Trefethen and D. Bau, *Numerical Linear Algebra, Twenty-fifth Anniversary Edition*. Philadelphia, PA: Society for Industrial and Applied Mathematics, 2022. doi: 10.1137/1.9781611977165.
- [25] A. Yalavarthi and B. Singh, "SMO-Based Position Sensorless SRM Drive for Battery-Supported PV Submersible Pumps," *IEEE Journal of Emerging and Selected Topics in Power Electronics*, vol. 10, no. 4, pp. 3917–3926, Aug. 2022, doi: 10.1109/JESTPE.2021.3067955.

BIOGRAPHIES OF AUTHORS

Carlos Vergara-Ramírez    received the B.Sc. degree in Control Engineering from the Universidad Distrital Francisco José de Caldas, Bogotá, Colombia, in 2013, and M.Sc. degree in Industrial Automation from the Universidad Nacional de Colombia, Bogotá, Colombia, in 2021. He is currently a full professor of Mechatronic Engineering at Escuela Tecnológica Instituto Técnico Central, Bogotá, Colombia. His research interests include the theoretical and practical aspects of automatic control and identification of mechatronic systems and electric machines. He can be contacted at email: cfvergarar@itc.edu.co.



John Cortés-Romero    he is an Electrical Engineer, Master in Industrial Automation and Master in Mathematics from the National University of Colombia (1995, 1999, and 2007, respectively). He has a Ph.D. in Sciences (2011), with a specialty in Electrical-Mechatronic Engineering from the CINVESTAV Institute of Mexico. Currently, he is a professor in the Department of Electrical and Electronic Engineering at the National University of Colombia. He can be contacted at email: jacortesr@unal.edu.co.



Horacio Coral-Enriquez    received the B.Sc. degree in Engineering in Industrial Automatica from the Universidad del Cauca, Popayán, Colombia, in 2005, and the M.Sc. degree in Automatica from the Universidad del Valle, Cali, Colombia, in 2010. In 2017 he received the Ph.D. degree (Cumlaude) from the Universidad Nacional de Colombia. Currently, he is a Research Associate Professor of the Faculty of Engineering at the Universidad de San Buenaventura, Bogotá, Colombia. He is the author of over 40 technical papers in journals and international conference proceedings. His main research areas include active disturbance rejection control, nonlinear control, wind turbine control, and applications of control theory. He can be contacted at email: hcoral@usbog.edu.co.